

Transmembrane Peptides Stabilize Inverted Cubic Phases in a Biphasic Length-Dependent Manner: Implications for Protein-Induced Membrane Fusion

D. P. Siegel,* V. Cherezov,[†] D. V. Greathouse,[‡] R. E. Koeppe II,[‡] J. Antoinette Killian,[§] and M. Caffrey^{†¶**}

*Givaudan Inc., Cincinnati, Ohio; [†]Department of Chemistry, The Ohio State University, Columbus, Ohio; [‡]Department of Chemistry and Biochemistry, University of Arkansas, Fayetteville, Arkansas; [§]Department of Biochemistry of Membranes, University of Utrecht, Utrecht, The Netherlands; [¶]Biochemistry and Biophysics Programs, The Ohio State University, Columbus, Ohio; and ^{**}College of Science, University of Limerick, Limerick, Ireland

ABSTRACT WALP peptides consist of repeating alanine-leucine sequences of different lengths, flanked with tryptophan “anchors” at each end. They form membrane-spanning α -helices in lipid membranes, and mimic protein transmembrane domains. WALP peptides of increasing length, from 19 to 31 amino acids, were incorporated into *N*-monomethylated dioleoylphosphatidylethanolamine (DOPE-Me) at concentrations up to 0.5 mol % peptide. When pure DOPE-Me is heated slowly, the lamellar liquid crystalline (L_α) phase first forms an inverted cubic (Q_{II}) phase, and the inverted hexagonal (H_{II}) phase at higher temperatures. Using time-resolved x-ray diffraction and slow temperature scans (1.5°C/h), WALP peptides were shown to decrease the temperatures of Q_{II} and H_{II} phase formation (T_Q and T_H , respectively) as a function of peptide concentration. The shortest and longest peptides reduced T_Q the most, whereas intermediate lengths had weaker effects. These findings are relevant to membrane fusion because the first step in the L_α/Q_{II} phase transition is believed to be the formation of fusion pores between pure lipid membranes. These results imply that physiologically relevant concentrations of these peptides could increase the susceptibility of biomembrane lipids to fusion through an effect on lipid phase behavior, and may explain one role of the membrane-spanning domains in the proteins that mediate membrane fusion.

INTRODUCTION

WALP peptides are hydrophobic, α -helical transmembrane peptides that incorporate into lipid bilayers (1–5). The helical axes of such peptides are nearly perpendicular to the plane of the membrane at room temperature (1,3,4,6–8) and the core of the helices, when membrane-embedded, is strongly protected from solvent deuterium exchange (9). Because of these properties, WALP peptides are models for the single helical membrane-spanning domains found in some integral membrane proteins (1,4). WALP peptides stabilize inverted phases in phospholipids in a peptide-length- and concentration-dependent fashion. In previous studies, peptides whose lengths as rigid α -helices are short compared to the thickness of the lamellar phase bilayer of the host lipid were generally found to be effective in inducing nonlamellar phase formation, with the concentration required depending on the nature of the lipids. For example, it was shown that high concentrations of short WALP peptides (~10 mol %) can induce formation of H_{II} and so-called isotropic phases in fully hydrated phosphatidylcholine systems (1–3), which only form the lamellar liquid crystalline (L_α) phase in the absence of the peptides. Peptide concentrations of 1–4 mol % can substantially lower the L_α/H_{II} transition temperature and induce formation of an inverted cubic (Q_{II}) phase in 1,2-diacyldioyl-*sn*-3-glycerol-3-phosphoethanolamine (DEPE) (10).

WALP concentrations as small as 0.1 mol % substantially lowered the temperature for isotropic phase formation in a 1,2-dioleoyl-*sn*-glycerol-3-phosphoethanolamine/1,2-dioleoyl-*sn*-glycerol-3-phosphoglycerol (DOPE/DOPG) mixture (11). Also, in previous studies, WALP peptides with lengths longer than the host lipid bilayer thickness were found to have little or no effect (10,11) on the phase behavior of the lipids. The fact that WALP peptides and other transmembrane peptides (12) can stabilize nonlamellar (H_{II} and Q_{II}) phases is especially interesting in light of the association of inverted phase behavior with membrane fusion (see, e.g., Ellens et al. (13) and Siegel (14)) and the possible influence of inverted phase behavior on membrane protein function (reviewed in Eppand (15)).

This work deals with the influence of WALP peptides on the formation of Q_{II} and H_{II} phases from the L_α phase in DOPE-Me. These experiments were motivated by an interest in the physical chemical mechanisms by which proteins induce biomembrane fusion, which are still poorly understood. There is a close relationship between Q_{II} phase formation and the occurrence of membrane fusion in some pure lipid systems. Simply stated, formation of membrane fusion pores is postulated to be the first step in the L_α/Q_{II} phase transition (14,16). Membrane fusion rates increase substantially as unilamellar vesicle dispersions of DOPE-Me and DOPE/1,2-dioleoyl-*sn*-glycerol-3-phosphocholine lipid mixtures are incubated at increasing temperatures in the region where Q_{II} phase precursors and Q_{II} phases are detected by ³¹P NMR and freeze-fracture electron microscopy

Submitted July 11, 2005, and accepted for publication September 13, 2005.

Address reprint requests to David P. Siegel, Givaudan Inc., 1199 Edison Drive, Cincinnati, OH 45215. Tel.: 513-948-4840; E-mail: david.siegel@givaudan.com.

© 2006 by the Biophysical Society

0006-3495/06/01/200/12 \$2.00

doi: 10.1529/biophysj.105.070466

(13). The Q_{II} precursors are catenoidal connections (interlamellar attachments) with central water channels that form between lamellae (17–19). These connections, formed between unilamellar liposomes, would achieve fusion between the liposomes (nonleaky continuity of both the liposomal membranes and aqueous contents). Siegel et al. (17,18) showed that the connections formed in unilamellar liposomal dispersions in the same temperature region as the observed increases in membrane fusion rates (13), and that they formed lattices closely resembling the lattices of catenoidal intermediates proposed earlier (20) as precursors to Q_{II} phase formation (21). Thus, one can study physical chemical influences on the fusion rate in model membrane systems by determining whether given changes in composition or conditions alter the onset temperature for the L_α/Q_{II} phase transition (T_Q). A number of authors have exploited this relationship in studying the effects of small peptides and lipid additives on membrane fusion in DOPE-Me (see, e.g., Yeagle et al. (22), Epand and Epand (23), Epand et al. (24), Nieva et al. (25), Davies et al. (26), and Basáñez et al. (27)). DOPE-Me is an appropriate choice of lipid for such studies because, at slow temperature scan rates (e.g., 1.5°C/h), it has a well characterized L_α/Q_{II} phase transition that begins at ~59.6°C (28).

There is increasing evidence that membrane-spanning domains are important for activity of proteins that mediate membrane fusion (reviewed in Schroth-Diez et al. (29)). Moreover, peptides corresponding to the membrane-spanning domains of these proteins fuse liposomes in the absence of other peptides or proteins (30–33). The only domains of the fusion-mediating protein in influenza virus that have been demonstrated to closely associate with the lipids of target and host membrane lipids under fusogenic conditions are the so-called fusion peptides and the membrane-spanning domains of the same protein (34). The interactions of fusion peptides with lipids have been studied extensively for almost two decades (35) (for reviews, see Nieva and Agirre (36), Tamm et al. (37,38), and Martin et al. (39)), whereas biophysical characterization of the membrane-spanning domains of fusion proteins and their activity in liposome fusion started more recently (30–33,40).

In this study, we used time-resolved x-ray diffraction (TRXRD (41)) to determine the changes in lipid phase behavior (and especially changes in T_Q) induced by adding WALP peptides to DOPE-Me. By using TRXRD and a host lipid with a well defined T_Q (28), we can determine the effects of different peptides on Q_{II} phase formation with greater precision than in previous studies (see, e.g., van der Wel et al. (10), Morein et al. (11), and Liu et al. (12)). Also, TRXRD directly verifies the presence of Q_{II} phases, whereas other methods, such as ³¹P NMR, cannot distinguish between Q_{II} phases and Q_{II} phase precursors. In light of recent theoretical work (16), the results allow us to estimate the effects that such membrane-spanning peptides have on the stability of fusion pores. It can be shown (16) that 1 mol % of

a particular WALP peptide would lower the energy of fusion pores in a lipid such as DOPE-Me by as much as 40 $k_B T$.

MATERIALS AND METHODS

Materials

Buffers and reagents

Buffers and reagents were as described in Cherezov et al. (28).

WALP peptide synthesis

Table 1 shows the sequences of the peptides used in this study. The peptides were prepared by fluorenylmethoxycarbonyl (Fmoc) solid-phase methods on an ABI 433A peptide synthesizer (PE Biosystems, Foster City, CA). The Fmoc amino acids, from Advanced ChemTech (Louisville, KY) or Bachem Bioscience (King of Prussia, PA), were coupled as hydroxybenzotriazol esters in the presence of [2-(1 *H*-benzotriazol-1-yl)-1,1,2,3-tetramethyluronium hexafluorophosphate] to a preloaded Fmoc-L-Ala Wang resin (Advanced ChemTech). All peptide synthesizer reagents were purchased from PE Biosystems except dichloromethane and *N*-methylpyrrolidinone, which were high-performance liquid chromatography (HPLC)-grade obtained from Allied Signal (Muskegon, MI). Occasional failure sequences, due to incomplete coupling of a particular hydrophobic amino acid, were capped using acetic anhydride; this precaution was important to prevent the accumulation of significant amounts of (n-1) or (n-2) peptides. Fmoc-deprotection at each step was with piperidine/*N*-methylpyrrolidinone (1:4 v/v). The synthesis was completed by coupling acetyl-Gly (Advanced ChemTech), also as the hydroxybenzotriazol ester. The completed peptides were cleaved from the resin with 20 vol % distilled ethanolamine (Aldrich Chemical, Milwaukee, WI) in dichloromethane for 48 h at 25°C (42). The peptides were lyophilized to a white powder from trifluoroethanol (TFE)/water (1:1 v/v). Based on analytical HPLC, the purity of the peptides was 80–95%.

Some batches of WALP 19, 23, 27, and 31 were further purified via reversed-phase HPLC. These will be referred to as purified peptides. Samples of WALP19, WALP23, and WALP27 were dissolved in TFE (50 mg/mL) and purified on a Zorbax SB-C8 semipreparative column using a solvent gradient of methanol and 0.1 vol % trifluoroacetic acid in deionized water. After purification, the peptides were lyophilized to a white powder from TFE/deionized water (50:50 v/v) as described above, and their purity was estimated to be 98% by analytical reversed-phase HPLC analysis and electrospray mass spectral analysis. Due to its length, WALP31 was HPLC-purified using a Nucleosil column (SI 100-10, pore size 100 Å), obtained from Macherey-Nagel (Düren, Germany) with chloroform/methanol/water (80:19:1 v/v) as eluent, and then lyophilized to a white powder, ~98% pure. HPLC purification of these very hydrophobic peptides results in a large peptide loss, presumably because of aggregate formation.

TABLE 1 Sequences and lengths of the WALP peptides used

Peptide	Sequence	Length as an α -helix (Å)*
WALP19	Ac-GWW-(LA) ₆ L-WWA-e	28.5
WALP23	Ac-GWW-(LA) ₈ L-WWA-e	34.5
WALP25	Ac-GWW-(LA) ₉ L-WWA-e	37.5
WALP27	Ac-GWW-(LA) ₁₀ L-WWA-e	40.5
WALP31	Ac-GWW-(LA) ₁₂ L-WWA-e	46.5

Ac, acetyl; e, ethanolamine; A, alanine; G, glycine; L, leucine; and W, tryptophan.

*The helix length was calculated by multiplying the number of residues by 1.5 Å.

DOPE-Me

N-monomethylated 1,2-dioleoyl-*sn*-glycero-3-phosphoethanolamine (DOPE-Me) was used as received from Avanti Polar Lipids (Alabaster, AL), as lyophilized powder. All the DOPE-Me used in this study was from the same lot that was used in studies of the L_α/Q_{II} transition in pure DOPE-Me (28). Lipid received from the manufacturer was stored at -70°C until samples were prepared for x-ray diffraction experiments.

Methods

DOPE-Me/peptide samples

Peptides were mixed with DOPE-Me using a TFE/water lyophilization technique developed previously (1). WALP peptide stock solutions (0.3–3.4 mg/mL, depending on the peptide and the desired concentration in the lipid) were made up in TFE. The WALP peptide concentration in the TFE stock solution was determined by the absorbance after dilution with methanol (final methanol concentration $>95\%$ v/v) at 280 nm, using blank solutions of the same TFE/methanol ratio. The molar extinction coefficient of *N*-tertiary butyloxycarbonyl L-tryptophan at 280 nm was determined in methanol as $5590\text{ M}^{-1}\text{ cm}^{-1}$ (data not shown). Since there are four tryptophan residues in each WALP peptide, we used a molar extinction coefficient of $22,400\text{ M}^{-1}\text{ cm}^{-1}$ for all the peptides. An appropriate amount of lyophilized DOPE-Me as received from the supplier was weighed into a Pyrex flask and hydrated with 0.25 mL of Milli-Q water by vortex mixing. A 0.25-mL of WALP peptide stock solution of appropriate concentration in TFE was added to the hydrated DOPE-Me with vortex mixing, diluted with 3.75 mL of water with vortex mixing on ice, frozen in liquid nitrogen, and then lyophilized. Lyophilized samples were hydrated in 150 mM NaCl, 20 mM *N*-tris[Hydroxymethyl]methyl-2-aminoethane-sulfonic acid, 0.1 mM EDTA, pH 7.4, by vortex mixing under Ar and equilibrating on ice for 1 h, after which they were subjected to six freeze/thaw cycles (dry ice/room temperature water). Peptide concentrations are given in units of mol % ($100 \times \text{moles of peptide}/(\text{moles of peptide} + \text{moles of DOPE-Me})$). The error in peptide concentration in each sample is estimated to be $\pm 5\%$.

X-ray diffraction samples

Samples were prepared as described previously (28). Capillaries were stored in closed, screw-capped test tubes at -70°C until they were used (generally less than two weeks). Values of T_Q obtained on single sets of samples observed after different times of storage at -70°C were the same to within the reproducibility of the measurement (1°C) for samples stored for at least 35 days. Values of T_Q determined by rotating anode x-ray diffraction experiments with samples made using different preparations of the same WALP peptide were the same to within 2°C after storage times of 1–35 days.

Rotating anode and synchrotron source x-ray diffraction measurements

These measurements were performed using the same apparatus and methods described in detail in (28), with the following exceptions. In the synchrotron-source experiments, a monochromatic x-ray beam of either 8.979 keV (wavelength 1.38 Å) or 8.045 keV (wavelength 1.54 Å) was focused at a detector position of 125.5 cm (8.979 keV) or 112.0 cm (8.045 keV), as was determined using a silver behenate standard (43). The temperature in the sample cell was determined using thermocouples inserted into sample capillaries, and was correct to within 0.2°C versus NBS-traceable standards (28). Samples were incubated for 1 h at the starting temperature before any of the experiments commenced. During temperature-scan experiments diffraction patterns were collected using 1-min exposures and at 8-min intervals, at a scan rate of 1.5°C/h . These correspond to intervals of 0.2°C , and to changes in temperature of 0.025°C during each exposure. One data set

(0.5 mol % WALP27 in DOPE-Me) was obtained at a scan rate of 2°C/h , with 1-min exposures every 7.5 min (exposures at intervals of 0.25°C). All temperature-scan experiments were performed in the heating direction. The temperature range examined for all peptides extended to 12°C above T_Q . In temperature-jump experiments, twenty 1-min exposures were collected in succession, followed by eight 1-min exposures at intervals of 5 min and three or more 1-min exposures at intervals of 10 min. The x-ray shutter was closed during the idle time between exposures to minimize radiation damage (28,44,45).

Radiation damage study

A radiation damage study protocol very similar to that described for experiments with pure DOPE-Me (28) was followed. Using NSLS beamline X-12B (8.979 keV), we exposed a capillary containing 0.5 mol % WALP31 in DOPE-Me continuously for 1 h at 35°C . This temperature is $\sim 3^\circ\text{C}$ below the temperature at which Q_{II} phases first formed from the L_α phase in a sample of the same preparation, as determined from a previous rotating anode temperature-scan experiment. As with the sample of pure DOPE-Me treated in the same way at 57°C (28), 60 successive 1-min exposures were made while the sample was in the x-ray beam, and patterns obtained during this time showed the presence of only lamellar phase. Immediately after the 60-min irradiation, 1-min exposures were used to collect diffraction patterns from adjacent, unirradiated regions of the same sample. As with the pure DOPE-Me sample (28), the intensity of the lamellar phase diffraction peaks decreased with time throughout the irradiation, and decreased slightly in the displaced patterns (obtained 12–20 min after the end of the experiment) versus the final pattern obtained during the 60-min irradiation. As discussed in Cherezov et al. (28), this continuous decrease also occurs in DOPE-Me samples irradiated only intermittently and DOPE-Me samples examined with much weaker rotating-anode x-ray sources (see, e.g., Gruner et al. (46)). Since the Q_{II} phase was not observed in the 0.5 mol % WALP31 sample irradiated for 60 min, we conclude that the radiation doses used in these experiments had no effect or very minor effects on the observed transition temperatures and lipid phase behavior.

RESULTS

TRXRD experiments

Previously, we showed that, when heated at a scan rate of 1.5°C/h , DOPE-Me forms a Q_{II} phase starting at $59.6 \pm 0.6^\circ\text{C}$, and then the H_{II} phase (to coexist with the Q_{II} phase) starting at $63.7 \pm 0.4^\circ\text{C}$ (28). The inclusion of WALP peptides alters these temperatures. An example of synchrotron TRXRD data is given in Fig. 1, which shows a diffraction pattern obtained with 0.2 mol % WALP19 in DOPE-Me at 53°C . It was collected as part of a series as the sample was heated from 44.7 to 54.9°C at 1.5°C/h . This pattern was chosen because it shows the simultaneous presence of diffraction rings from the Q_{II} -Pn3m, H_{II} , and L_α phases during a series of phase transitions from the lamellar phase. WALP-containing samples were examined using slow temperature scans because the L_α/Q_{II} phase transition in pure DOPE-Me is very slow (hours) and hysteretic (21,28). A direct L_α/Q_{II} phase transition is detected in pure DOPE-Me only when the temperature scan rate is $<3^\circ\text{C/h}$, and the observed transition temperature is nearly constant with decreasing scan rate at $\leq 1.5^\circ\text{C/h}$ (28). Therefore, we used a scan rate of 1.5°C/h in our rotating-anode and

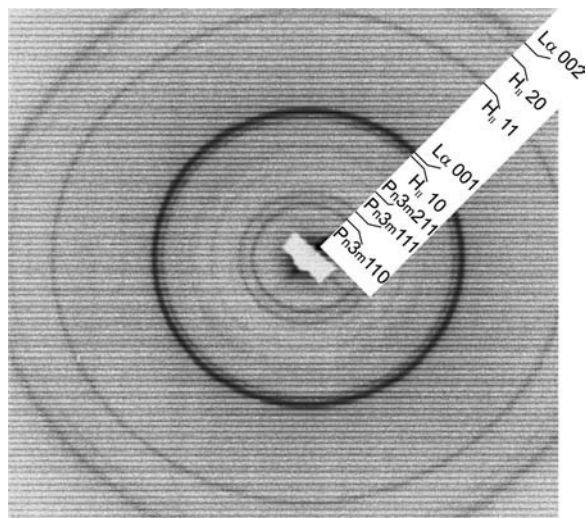


FIGURE 1 Typical two-dimensional detector image of a diffraction pattern from 0.2 mol % WALP19 in DOPE-Me at 53°C recorded using synchrotron radiation. This pattern was obtained in a 1-min exposure as described in Cherezov et al. (28), as part of a series as the sample was heated from 44.7°C to 54.9°C at a scan rate of 1.5°C/h. This pattern shows the presence of diffraction rings from Q_{II}-(Pn3m), H_{II}, and L_α phases, as labeled in the figure. The Q_{II}-Pn3m (110) reflection and L_α (002) reflections are at 174 Å and 31.1 Å, respectively.

synchrotron experiments to avoid possible ambiguities in phase behavior. Formally, for the Q_{II} phases noted as Q_{II}-Pn3m in this work, we cannot distinguish between the space groups Pn3m and Pn3 (47). Harper et al. state that these cannot be distinguished on the basis of powder patterns alone (48).

Transition temperatures as determined by TRXRD experiments

T_Q and T_H are the onset temperatures for formation of the Q_{II} and H_{II} phases, respectively. Lamellar and nonlamellar phases coexisted over temperature intervals of between 3° and 10°. Fig. 2 summarizes the rotating-anode TRXRD transition temperature data on WALP/DOPE-Me systems. The plots in Fig. 2 show the dependence of T_Q and T_H on the concentration of WALP peptide for four peptides: WALP19, WALP23, WALP27, and WALP31. As for pure DOPE-Me (28), T_Q was determined as the temperature at which the first low-angle reflections (corresponding to spacings of ~220 Å) appeared. The presence of Q_{II} phases under these conditions was verified by synchrotron source temperature scan-experiments, which will be discussed below. For different capillaries made from the same WALP/DOPE-Me sample, the reproducibility of T_Q as determined from rotating anode streak-camera images was generally to within $\pm 1^\circ\text{C}$. For capillaries made from different samples of the same WALP peptide, the reproducibility was $\pm 2.5^\circ\text{C}$ or less. Therefore different samples of the same peptide had the same efficacy in lowering T_Q to within the error of the measurements.

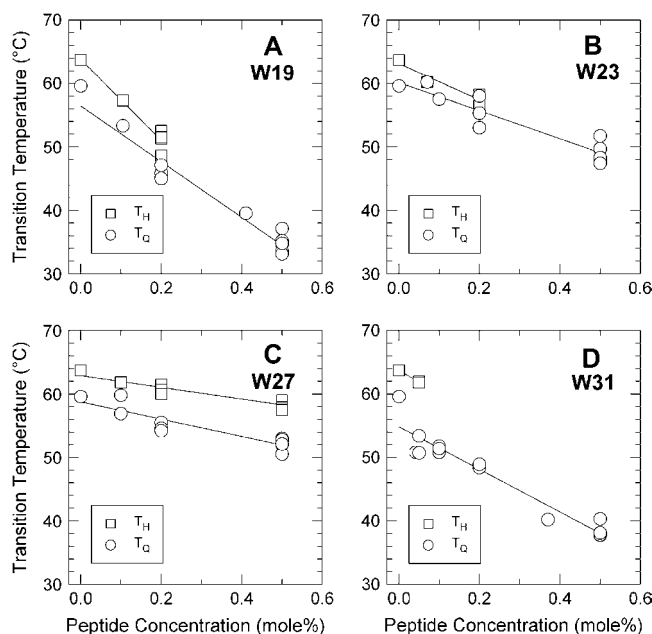


FIGURE 2 Effects of WALP peptides on the onset temperatures for formation of Q_{II} (T_Q) and H_{II} phases (T_H) in DOPE-Me as a function of peptide length and concentration, as determined via rotating-anode TRXRD experiments. The lines in the plots are linear regression fits to the data. The correlation coefficients for the plots of T_Q and T_H , respectively, are (A) 0.954 and 0.944; (B) 0.887 and 0.911; (C) 0.791 and 0.883; and (D) 0.925 and 0.991. The fits included the data at zero concentration. The T_Q value at zero peptide concentration ($59.6 \pm 0.6^\circ\text{C}$; pure DOPE-Me) represented six measurements. In the case of WALP31, the intercept of the T_Q line with the temperature axis is 4.8°C below T_Q for pure DOPE-Me.

The data in Fig. 2 show that all the WALP peptides lower T_Q and T_H , which for the pure lipid under these conditions are $59.6 \pm 0.6^\circ\text{C}$ and $63.7 \pm 0.4^\circ\text{C}$, respectively (28). Both T_Q and T_H decrease linearly with increasing peptide concentration over most of the concentration range. The extent of the effects on T_Q and T_H depends on the length of the WALP peptide.

The slopes of the plots of T_Q versus peptide concentration are $-45^\circ\text{C/mol } \%$, $-22^\circ\text{C/mol } \%$, $-13^\circ\text{C/mol } \%$, and $-34^\circ\text{C/mol } \%$ for WALP19, WALP23, WALP27, and WALP31, respectively. This shows that the shortest (WALP19) and longest (WALP31) peptides are most effective in reducing T_Q , whereas the intermediate-length peptides have more modest effects. Measurements of T_Q were also made for samples containing 0.5 mol % of the peptide WALP25. From these measurements, a value of T_Q of $53.6 \pm 1.3^\circ\text{C}$ (average of four determinations) was determined. The peptide-length-dependent effects on T_Q evaluated at 0.5-mol % peptide concentration are summarized in Fig. 3. The data for the pure hydrated DOPE-Me represents the average of six trials ($59.6^\circ\text{C} \pm 0.6^\circ\text{C}$).

In control experiments using 0.5 mol % of purified WALP19, WALP23, WALP27, and WALP31 (Fig. 3), the purified peptides (*open circles*) lowered the T_Q of DOPE-Me

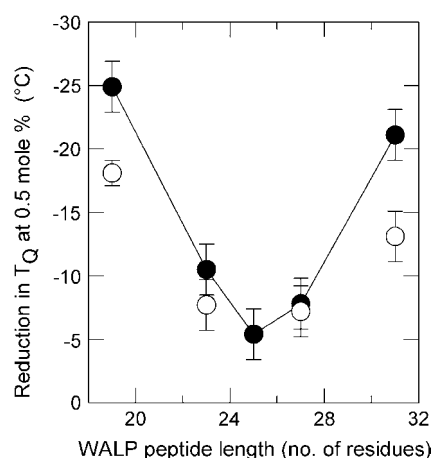


FIGURE 3 Summary of the effects of WALP peptides on T_Q as a function of WALP peptide sequence length. The plot shows the extent of reduction in T_Q at a peptide concentration of 0.5 mol % for each WALP peptide examined in this study. The data are plotted in this fashion to facilitate comparison of the purified WALP peptides and WALP25, which were studied only at a concentration of 0.5 mol %, with the data for the peptides in Fig. 2. (●) Nonpurified peptides. (○) Purified peptides.

with qualitatively similar length dependence as the non-purified peptides (*solid circles*). However, the extent of reduction in T_Q for each WALP length was smaller for the purified peptides, in particular for the shortest and longest peptides.

The effects of the peptides on T_H were rather similar to those on T_Q . The slopes of the plots of T_H versus peptide concentration are $-64^\circ\text{C/mol } \%$, $-29^\circ\text{C/mol } \%$, $-8^\circ\text{C/mol } \%$, and $-36^\circ\text{C/mol } \%$ for WALP19, WALP23, WALP27, and WALP31, respectively, showing that the shortest (WALP19) and longest (WALP31) peptides are most effective in reducing T_H . For samples containing 0.5 mol % of WALP25, T_H was found to be $58.2 \pm 0.3^\circ\text{C}$. Thus, WALP25 only has a small effect on T_H , rather similar to that of WALP27.

At relatively high peptide concentrations of 0.5 mol %, H_{II} phases were observed only for WALP27 and WALP25, at $\sim 5^\circ\text{C}$ above T_Q (Fig. 2 C). Pure DOPE-Me forms the H_{II} phase at $\sim 4^\circ\text{C}$ above T_Q when examined in similar slow temperature-scan heating experiments. Thus, WALP25 and WALP27 perturb the phase behavior of DOPE-Me less than the other WALP peptides.

Synchrotron source temperature-scan experiments were performed on eight of the WALP/DOPE-Me compositions, to refine the measurements of T_Q , determine which Q_{II} phases formed, and study the behavior of the Q_{II} phase lattice constants with temperature and time after temperature jumps. An example of the synchrotron TRXRD data on Q_{II} phase formation is shown in Fig. 4 A, for 0.5 mol % WALP31 in DOPE-Me. In this experiment, the sample was heated continuously from 35.0°C to 39.0°C , at 1.5°C/h . The only peaks in the 35.0°C pattern correspond to the first- and

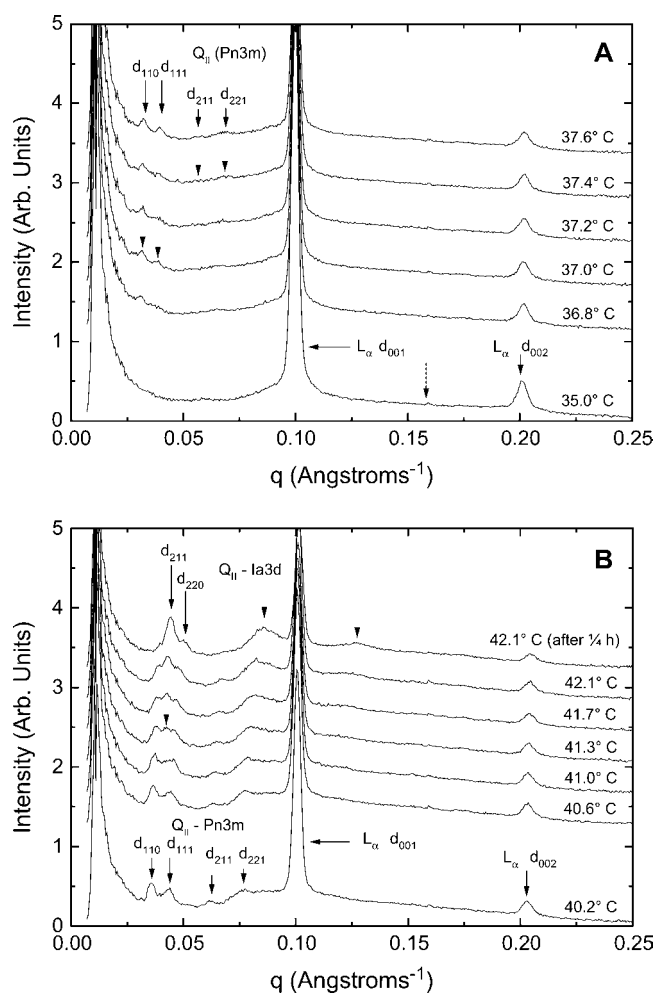


FIGURE 4 Results of synchrotron temperature-scan experiments using 0.5 mol % WALP31 in DOPE-Me, showing formation of Q_{II} phases. The curves are the radial integrals of two-dimensional diffraction patterns like the one in Fig. 1, taken at temperature intervals of 0.2°C . The ordinate is the diffracted intensity, and the abscissa is the magnitude of the scattering vector $q = 2\pi/d$, where d is the interplane spacing in \AA . (A) Diffraction patterns from an experiment in which the temperature was increased continuously at 1.5°C/h , from 35.0°C to 39.0°C . The only peaks in the 35.0°C pattern are the indicated reflections from the L_α phase. At 37.0°C , two peaks appear at $q = \sim 0.032$ and 0.038 \AA^{-1} (arrowheads). At 37.4°C , two more small peaks appear at $\sim 0.057 \text{ \AA}^{-1}$ and 0.069 \AA^{-1} (arrowheads). In the pattern at 37.6°C , the four new peaks are labeled as the indicated reflections from a Q_{II} -Pn3m phase. (B) Diffraction patterns obtained from another sample of 0.5 mol % WALP31 in DOPE-Me, heated at 1.5°C/h between 37.0°C and 42.1°C . The pattern at 40.2°C shows the same Q_{II} -Pn3m and L_α phase reflections as the 37.6°C pattern in A. A new peak at $q = 0.042 \text{ \AA}^{-1}$ became clearly visible in the 41.3°C data (arrowhead). In the pattern at 42.1°C , this peak had grown in intensity at the expense of the Q_{II} -Pn3m reflections. The plot at the top of the figure was obtained 15 min after the end of the scan, with the temperature constant at 42.1°C . Additional peaks are visible in this pattern (arrowheads). The two peaks indicated by arrows index as the first two (211 and 220) reflections of a Q_{II} -Ia3d phase. The higher- q peaks likely correspond to the superposition of multiple reflections, and could not be reliably indexed. Dashed arrow in A: the very small feature in the baseline at $q = 0.159 \text{ \AA}^{-1}$ is due to a flaw in the detector, and does not represent a diffraction peak.

peak at $q = 0.127 \text{ \AA}^{-1}$ may represent high-order reflections from the Q_{II} -Ia3d phase.

In Fig. 4 *B*, the two reflections at $q = 0.042 \text{ \AA}^{-1}$ and 0.05 \AA^{-1} (observed at temperatures $\geq 41.3^\circ\text{C}$ and 42.1°C , respectively) are too weak and too few in number to rigorously identify the new lattice. However, we tentatively identify this higher-temperature Q_{II} lattice as the Q_{II} -Ia3d phase, based on the ratio of the apparent Q_{II} -Pn3m and Q_{II} -Ia3d lattice constants. Fig. 5 *A* shows plots of the lattice constants of the two Q_{II} phases as a function of temperature for the experiment in Fig. 4 *B*. Fig. 5 *B* shows that the ratio of the Q_{II} -Ia3d and Q_{II} -Pn3m lattice constants over the entire temperature range is centered at 1.54, close to the value of 1.58 expected for coexisting Q_{II} -Ia3d and Q_{II} -Pn3m lattices (49,50). The putative Q_{II} -Ia3d phases were observed in synchrotron experiments at temperatures between 2° and 9°C above T_Q in the WALP peptide systems (Table 2). The diffracted intensity from this phase grew at the expense of diffraction from the Q_{II} -Pn3m phase with increasing temperature.

Q_{II} -Ia3d phase formation is sensitive to the temperature history of the sample. The Q_{II} -Ia3d phase did not always

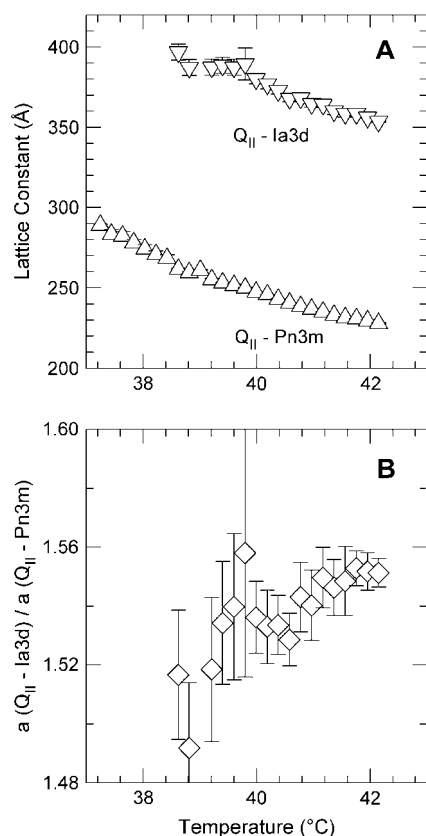


FIGURE 5 Lattice constants and lattice constant ratio of the Q_{II} phases detected by the synchrotron TRXRD experiment in Fig. 4, as a function of temperature, for 0.5 mol % WALP31 in DOPE-Me. (A) Dependence of the lattice constants of the Q_{II} -Pn3m and Q_{II} -Ia3d phases on temperature. (B) Dependence of the ratio of the Q_{II} -Ia3d and Q_{II} -Pn3m lattice constants on temperature. This ratio is close to the value of 1.58 expected for coexisting Q_{II} -Ia3d and Q_{II} -Pn3m lattices (49,50).

appear in temperature-jump experiments using samples of the same composition that would form Q_{II} -Ia3d phase in temperature-scan experiments. The samples subjected to temperature-jump experiments were 0.5 mol % WALP19, 0.5 mol % WALP23, and 0.5 mol % WALP31 (data not shown). We do not know the reasons for this difference between temperature-scan and temperature-jump experiments.

DISCUSSION

Reduction in T_Q and T_H in DOPE-Me by WALP peptides

The principal result of this study is that WALP peptides substantially lower the temperatures at which Q_{II} and H_{II} phases form in DOPE-Me in a peptide-length-dependent manner (Figs. 2 and 3). For most peptides, the extent of the decrease in T_Q and T_H is linear in peptide concentration (Fig. 2). At constant peptide concentration, the extent to which each peptide reduces T_Q and T_H depends on the peptide length. This peptide length dependence is biphasic (Fig. 3): both the shortest (WALP19) and longest (WALP31) peptides were most effective in reducing the transition temperatures, compared to the peptides of intermediate lengths. Qualitatively, the phase behavior of WALP/DOPE-Me systems in temperature-scan experiments resembles that of pure DOPE-Me (28), where the Q_{II} phase forms at a lower temperature than the H_{II} phase, and Q_{II} -Pn3m is the first Q_{II} phase to appear.

Comparison with other studies of WALP effects on nonlamellar phase formation

Two recent studies investigated the effects of WALP peptides on nonlamellar phase transition temperatures in DOPE/DOPG (11) and in DEPE (10). In both reports, Q_{II} phase formation was monitored primarily by observation of isotropic ^{31}P NMR resonances, with x-ray diffraction used to demonstrate formation of the Q_{II} phase under selected conditions. It should be noted that isotropic ^{31}P NMR resonances can arise from interlamellar attachments $10\text{--}15^\circ$ below T_Q in lipids such as DOPE-Me (e.g., for DOPE-Me, T_I in Ellens et al. (13) versus T_Q in Cherezov et al. (28)).

Most of our results are consistent with those of Morein et al. (11) and van der Wel et al. (10). First, WALP peptides lower the temperatures at which isotropic resonances are observed in each lipid system. Second, both van der Wel et al. and Morein et al. found that in the series WALP19–WALP31, shorter peptides were more effective than longer peptides in inducing formation of the isotropic phase. We found that the shorter peptides in the series WALP19–WALP25 reduced T_Q to a greater extent than did longer ones (Figs. 2 and 3). Third, van der Wel et al. (10) found that the shortest WALP peptides (WALP14 to WALP19) lowered the T_H of DEPE, whereas WALP21 and WALP23 had

smaller or vanishing effects. In qualitative agreement with this, we found that the shortest peptide (WALP19) was most effective in reducing T_H (Fig. 2). Finally, van der Wel et al. (10) found that 2 mol % of different-length WALP peptides had only a small effect (~ 1 Å or less) on the H_{II} tube diameter in DEPE at 60°C. We found that the peptides had even smaller effects (<0.2 Å) on lattice dimensions in DOPE-Me at a concentration of 0.5 mol % (data not shown).

Nevertheless, there is one important difference in our results. In DOPE-Me, we observed that WALP31 reduced T_Q to a significant extent. In contrast, in the studies by van der Wel and colleagues (10) and Morein et al. (11) it was found that WALP31 was less effective than shorter WALP peptides in inducing isotropic phase, perhaps due to a tendency of WALP31 to aggregate and phase-separate. In DOPE-Me, WALP31 does not phase-separate at concentrations up to 0.5 mol %; rather, it reduces T_Q to an extent that is nearly linear in peptide concentration in the range 0.05–0.5 mol % (Fig. 3 D). Nevertheless, our data do suggest that WALP31 also has a tendency to oligomerize. The plot of T_Q versus WALP31 concentration (Fig. 3 D) has a substantially larger apparent slope at concentrations <0.05 mol % than at higher concentrations. (We note a similar although less severe trend for WALP19 in Fig. 2 A.) Thus, at concentrations <0.05 mol % WALP31 appears to be present in a form that is more effective in reducing T_Q on a mole-for-mole basis than at higher concentrations. This suggests that at concentrations >0.05 mol % WALP31 shows a higher tendency than shorter analogs to form dimers or small aggregates.

A likely explanation for the peptide-length dependence of the phase behavior is that WALP peptides that are too long or too short to fit into the bilayer will disturb lipid packing in DOPE-Me in different ways, but with a similar result at relatively low peptide concentrations: a lowering of both T_Q and T_H .

In the case of the longer WALP31, the extent to which the system reacts by forming small aggregates of the peptide and cubic phases (as in DOPE-Me), versus more extensive aggregation and phase separation of the peptide (as in DEPE and PE/PG), seems to be very sensitive to the details of the particular system. The extent of hydrophobic mismatch should be comparable for a given WALP peptide in DOPE-Me (L_α phase bilayer thickness of 39 ± 5 Å; (46)), DOPE, DEPE, and DOPE/DOPG. It is therefore more likely that the differences in phase behavior of WALP31 in DOPE-Me as compared to the previous observations in DEPE and PE/PG are related to differences in the packing properties of the lipids in these systems. Since lipid packing is very different in the Q_{II} and H_{II} phases than in the L_α phase, it is interesting that T_Q and T_H are affected in the same way and to nearly the same extent by each peptide (Fig. 2). It may be that the peptides raise the free energy of the peptide-lipid L_α phase with respect to the pure lipid L_α phase more than they affect the free energy of the two inverted phases. This would have the effect of decreasing both T_H and T_Q in parallel as a function of peptide length, as is observed.

This explanation rationalizes most, but not all, of the data. Although T_H and T_Q are reduced by similar extents for all the peptides, the data in Fig. 2 show that H_{II} phase exists for different peptide concentration ranges for different WALP peptides. H_{II} phase is observed through 0.5 mol % for WALP27, but only through 0.2 mol % for WALP19 and WALP23, and only up until 0.05 mol % for WALP31. This could be due to nonequilibrium effects of the peptides on transition kinetics. However, different peptides may also be affecting the relative stability of Q_{II} and H_{II} phases differently. It has been pointed out that peptides could affect Q_{II} phase stability more than H_{II} phase stability if they change the monolayer Gaussian curvature elastic modulus of the lipids, κ (16,51). Different-length peptides are expected to affect κ differently, since this modulus is sensitive to the distribution of mass and intermolecular forces at different depths within the bilayer (52), and small changes in κ have a big influence on T_Q (16). Further studies of the effects of peptides on inverted phase stability (and especially on Q_{II} phase stability) are required to settle this question.

It has been suggested that membrane-spanning peptides could change T_H by effects on hydrophobic interstices (1) and T_Q by stabilization of differences in membrane thickness within the unit cells of the inverted phases (53). Interstice stabilization cannot explain the observed effects on T_Q . Q_{II} phases consist of continuous bilayers, with no hydrophobic interstices, so peptides cannot lower T_Q by packing interstices. More recent theoretical work (54,55) indicates that the chain-stretching energy associated with the bilayer thickness gradient in the Q_{II} phase is negligible for Q_{II} phases with unit cells as large as those observed in this study. The difference in free energy with respect to the L_α phase is due to a difference in bending elastic and Gaussian curvature energy (54,55). Thus the WALP peptides do not change T_Q via an effect on the chain-stretching energy of the Q_{II} phase.

It is likely that WALP peptides change T_H by stabilizing gradients in monolayer thickness in the H_{II} phases (1). These gradients are imposed by the necessity of filling hydrophobic interstices between H_{II} tubes. As discussed in Killian et al. (1), this could explain the effects of WALP peptides on T_H for peptides that are shorter than the L_α phase bilayer thickness (WALP19, WALP23, and WALP25 in this system). It is not clear that this principle explains the effects of peptides that have helices longer than the L_α phase bilayer thickness (WALP27 and WALP31). If membrane-spanning peptides form rigid rods, they must exist only in the regions of the H_{II} unit cell where the monolayers are opposed back-to-back, so that the two hydrophilic end groups of the peptide each reside in a lipid-water interface. These bilayer-like regions of the H_{II} phase are thinner than the bilayers in the L_α phase bilayer from which the H_{II} phase forms. Thus, there would be an increased extent of peptide-lipid length mismatch in the H_{II} versus the L_α phase for peptides like WALP27 and WALP31. This would increase T_H , rather than lower it, as we observed (Fig. 3, C and D). However, such

“long” membrane-spanning peptides might be able to lower T_H by filling hydrophobic interstices directly, if they can form kinks or bends. If the end groups of the peptide have to be in lipid-water interfaces, simple geometry shows that the peptide can fill an interstice if it can bend or kink in the middle by $\sim 30^\circ$. This might explain the efficacy of “long” peptides in reducing T_H . Interestingly, in peptides mimicking the membrane-spanning domains of some fusion-mediating proteins, activity in fusing pure lipid vesicles is correlated with increasing conformational flexibility of the peptides (30–33). Membrane fusion intermediates contain hydrophobic interstices (14,56). It may be that the more flexible peptides have the ability to form kinks, and act in part by filling the hydrophobic interstices within fusion intermediates in an analogous manner.

In addition to WALP peptides, other length-mismatched, transmembrane peptides can also influence lipid phase behavior. Recently, Liu et al. (12) studied the effects of peptides with polyleucine membrane-spanning domains and positively charged flanking residues on the T_H of DEPE and dipalmitaidoylphosphatidylethanolamine, and inferred the presence of Q_{II} phases from ^{31}P NMR data. In these experiments, transmembrane peptides longer than the PE membrane thickness also lowered T_H more than peptides with lengths approximately the same as the lipid membrane thickness. The results are very similar to our results comparing the effects of WALP31 versus shorter analogs on T_H and T_Q .

Implications for protein-mediated membrane fusion: influence of transmembrane domains

Proximity of biomembrane systems to the lamellar/nonlamellar phase boundary

Many biomembranes or biomembrane lipid extracts form nonlamellar phases if incubated above the physiological temperature (see, e.g., de Grip et al. (57), Burnell et al. (58), Gounaris et al. (59), Ranck et al. (60), Quinn et al. (61), and Lindblom et al. (62)), if dehydrated (see, e.g., Gruner et al. (63), Crowe and Crowe (65), and Gordon-Kamm and Steponkus (65)), or if treated with divalent cations (see, e.g., Cullis et al. (66), Albert et al. (67), Nicolay et al. (68), and Killian et al. (69)). Furthermore, the fusion rate in several lipid systems accelerates as one approaches the L_α/Q_{II} phase boundary, and the intermediates in membrane fusion correspond to intermediates in this phase transition. In some lipid extracts, Q_{II} phases or Q_{II} phase precursors are observed (62). More generally, Q_{II} phases should be stable in phospholipids in a broad temperature interval below T_H , although Q_{II} phase formation can be slowed or inhibited in some cases (14). Q_{II} phases even form in mixtures of unsaturated acyl-chain PC and cholesterol; two plasma membrane lipid components that cannot form inverted phases in excess water by themselves ((70,71); B. Tenchov,

R. C. MacDonald, and D. P. Siegel, unpublished). Under physiological conditions, the lipids of many biomembranes may be near the lamellar/ Q_{II} phase boundary. Addition of agents such as WALP-like transmembrane peptides that lower T_Q could therefore increase the tendency of the lipids to form fusion pore structures (Q_{II} phase precursors) between apposed membranes.

The transmembrane domains of proteins may facilitate membrane fusion

The membrane-spanning domains of viral fusion proteins appear to act by stabilizing nascent fusion pores at a post-hemifusion stage (see, e.g., Kemble et al. (72), Chernomordik et al. (73), Melikyan et al. (74), Razinkov et al. (75), Markosyan et al. (76), Melikyan et al. (77), Armstrong et al. (78), and Frolov et al. (79); for reviews, see Schroth-Diez et al. (29) and Earp et al. (80)). Moreover, peptides corresponding to the transmembrane domains of fusion-mediating proteins have been shown to induce liposome fusion in the absence of other peptides or proteins (30–33). The peptides in these studies acted at a posthemifusion stage, consistent with peptide action in stabilizing nascent fusion pores. In addition, peptides corresponding to mutants with reduced fusion activity in vivo were less active in stimulating fusion than the wild-type sequences.

In agreement with these results, this work also indicates that transmembrane peptides should increase the susceptibility of the lipids of membranes to membrane fusion. The peptides do so through an effect on the lipid phase behavior. Changes in lipid-peptide composition that stabilize Q_{II} phases relative to the L_α phase also stabilize fusion pores (16). We have shown that transmembrane WALP peptides substantially stabilize Q_{II} phases (lower T_Q) at concentrations of only 0.5 mol %, which is comparable to physiological conditions. For example, the fusion-mediating protein influenza hemagglutinin (HA) is present at a monomer concentration of 1.5 mol %, with each monomer having a single transmembrane domain (calculated using data from (81)). Transmembrane domains, if they have effects similar to those of WALP peptides on T_Q , could substantially accelerate fusion pore formation in biomembranes by a direct effect on the lipids. This is in addition to, or instead of, action of the domains through interactions with other regions of the fusion proteins. Our results indicate that domains that are either substantially longer or shorter than the thickness of the lipid bilayer should be especially effective (Table 1 and Fig. 3). If the membrane-spanning domains of fusion proteins are as effective as WALP19 in reducing T_Q in DOPE-Me, it can be shown that a local concentration 1.0 mol % of such domains would lower the energy of fusion pores by $\sim 40 k_B T$ (using data for DOPE-Me (16)).

The sequences of membrane-spanning domains affect their fusion activity, both in full-length proteins in vivo and in peptides in model membranes. For example, Langosch

58. Burnell, E., L. van Alphen, A. Verkleij, and B. de Kruijff. 1980. ³¹P nuclear magnetic resonance and freeze-fracture electron microscopy studies of *Escherichia coli*. *Biochim. Biophys. Acta*. 597:492–501.
59. Gounaris, K., D. A. Mannock, A. Sen, A. P. R. Brain, W. P. Williams, and P. J. Quinn. 1983. Polyunsaturated fatty acyl residues of galactolipids are involved in the control of bilayer/non-bilayer lipid transitions in higher plant chloroplasts. *Biochim. Biophys. Acta*. 732:229–242.
60. Ranck, J. L., L. Letellier, E. Shechter, B. Krop, P. Pernot, and A. Tardieu. 1984. X-ray analysis of the kinetics of *Escherichia coli* lipid and membrane structural transitions. *Biochemistry*. 23:4955–4961.
61. Quinn, P. J., A. P. R. Brain, L. C. Stewart, and M. Kates. 1986. The structure of membrane lipids of the extreme halophile, *Halobacterium cutirubrum*, in aqueous systems studied by freeze-fracture. *Biochim. Biophys. Acta*. 863:213–223.
62. Lindblom, G., I. Brentel, M. Sjolund, G. Wikander, and A. Wieslander. 1986. Phase behavior of membrane lipids from *Acholeplasma laidlawii*: importance of a single lipid forming nonlamellar phases. *Biochemistry*. 25:7502–7510.
63. Gruner, S. M., K. J. Rothschild, and N. A. Clark. 1982. X-ray diffraction and electron microscope study of phase separation in rod outer segment photoreceptor membrane multilayers. *Biophys. J.* 39: 241–251.
64. Crowe, L. M., and J. H. Crowe. 1982. Hydration-dependent hexagonal phase lipid in a biological membrane. *Arch. Biochem. Biophys.* 217:582–587.
65. Gordon-Kamm, W. J., and P. L. Steponkus. 1984. Lamellar-to-hexagonal_{II} phase transitions in the plasma membrane of isolated protoplasts after freeze-induced dehydration. *Proc. Natl. Acad. Sci. USA*. 81:6373–6377.
66. Cullis, P. R., B. de Kruijff, M. J. Hope, R. Nayar, A. Rietveld, and A. J. Verkleij. 1980. Structural properties of phospholipids in the rat liver inner mitochondrial membrane. A ³¹P NMR study. *Biochim. Biophys. Acta*. 600:625–635.
67. Albert, A. D., A. Sen, and P. L. Yeagle. 1984. The effect of calcium on the bilayer stability of lipids from bovine rod outer segment disk membranes. *Biochim. Biophys. Acta*. 771:28–34.
68. Nicolay, K., R. van der Neut, J. J. Fok, and B. de Kruijff. 1985. Effects of adriamycin on lipid polymorphism in cardiolipin-containing model and mitochondrial membranes. *Biochim. Biophys. Acta*. 819:55–65.
69. Killian, J. A., M. C. Koorengel, J. A. Bouwstra, G. Gooris, W. Dowhan, and B. de Kruijff. 1994. Effect of divalent cations on lipid organization of cardiolipin isolated from *Escherichia coli* strain AH930. *Biochim. Biophys. Acta*. 1189:225–232.
70. Epand, R. M., D. W. Hughes, B. G. Sayer, N. Borochoy, D. Bach, and E. Wachtel. 2003. Novel properties of cholesterol-dioleoylphosphatidylcholine mixtures. *Biochim. Biophys. Acta*. 1616:196–208.
71. Epand, R. M., R. F. Epand, A. D. Bain, B. G. Sayer, and D. W. Hughes. 2004. Properties of polyunsaturated phosphatidylcholine membranes in the presence and absence of cholesterol. *Magn. Reson. Chem.* 42:139–147.
72. Kemble, G. W., T. Danieli, and J. M. White. 1994. Lipid-anchored influenza hemagglutinin promotes hemifusion, not complete fusion. *Cell*. 76:383–391.
73. Chernomordik, L. V., L. Eugenia, M. M. Kozlov, V. A. Frolov, and J. Zimmerberg. 1999. Structural intermediates in influenza hemagglutinin-mediated fusion. *Mol. Membr. Biol.* 16:33–42.
74. Melikyan, G. B., S. Lin, M. G. Roth, and F. S. Cohen. 1999. Amino acid sequence requirements of the transmembrane and cytoplasmic domains of influenza virus hemagglutinin for viable membrane fusion. *Mol. Biol. Cell*. 10:1821–1836.
75. Razinkov, V. I., G. B. Melikyan, and F. S. Cohen. 1999. Hemifusion between cells expressing hemagglutinin of influenza virus and planar membranes can precede the formation of fusion pores that subsequently fully enlarge. *Biophys. J.* 77:3144–3151.
76. Markosyan, R. M., F. S. Cohen, and G. B. Melikyan. 2000. The lipid-anchored ectodomain of influenza virus hemagglutinin (GPI-HA) is capable of inducing nonenlarging fusion pores. *Mol. Biol. Cell*. 11:1143–1152.
77. Melikyan, G. B., R. K. Markosyan, M. G. Roth, and F. S. Cohen. 2000. A point mutation in the transmembrane domain of hemagglutinin of influenza hemagglutinin stabilizes a hemifusion intermediate that can transit to fusion. *Mol. Biol. Cell*. 11:3765–3775.
78. Armstrong, R. T., A. S. Kushnir, and J. M. White. 2000. The transmembrane domain of influenza hemagglutinin exhibits a stringent length requirement to support the hemifusion to fusion transition. *J. Cell Biol.* 151:425–437.
79. Frolov, V. A., M. S. Cho, P. Bronk, T. S. Reese, and J. Zimmerberg. 2000. Multiple local contact sites are induced by GPI-linked influenza hemagglutinin during hemifusion and flickering pore formation. *Traffic*. 1:622–630.
80. Earp, L. J., S. E. Delos, H. E. Park, and J. M. White. 2004. The many mechanisms of viral membrane fusion proteins. *Curr. Top. Microbiol. Immunol.* 285:25–66.
81. Lamb, R. A., and R. M. Krug. 1996. Orthomyxoviridae: the viruses and their replication. In *Virology*, Vol. 1. B. N. Fields, D. M. Knirpe, and P. M. Howley, editors. Lippincott-Raven, Philadelphia. 1353–1395.
82. Wimley, W. C., and S. H. White. 1996. Experimentally determined hydrophobicity scale for proteins at membrane interfaces. *Nature. Struct. Biol.* 3:842–848.